

Enriched Diagnosis of Osteoporosis using Deep Learning Models

Saumya Kumar, Puneet Goswami, and Shivani Batra*

Department of Computer Science and Engineering, SRM University, Sonipat, India

Abstract

Billions of people all over the globe suffer from osteoporosis, the second most prevalent bone condition after arthritis. Osteoporosis is brought on by a decline in bone mineral density, which can cause discomfort, deformity, injuries, and, in extreme instances, fatalities. Although DXA is used to diagnose it, its high price, limited availability, and erratic BMD values make it unreliable. The diagnoses have significantly improved owing to computer-aided diagnosis. A precise diagnosis of the condition may be made using deep learning-based networks, which have demonstrated cutting-edge outcomes in the diagnostic sector. Under the transfer learning methodology, this research investigates the performance of known neural network designs with the objective of osteoporosis diagnosis. The ability to distinguish between x-rays of healthy individuals and those obtained from individuals with osteoporosis has been tested using eight well-known ImageNet pre-trained models to provide a thorough comparison. 372 X-rays, divided into training and test sets, in the investigations. Standard evaluation parameters (such as accuracy, precision, recall and f1-score) have been calculated for all architectures, and the majority of designs performed significantly well, with the highest achieving an average accuracy of up to 86.36% when distinguishing the specified classes.

Keywords: convolutional neural network; diagnosis; knee; osteoporosis; transfer learning models; x-rays

© 2023 Totem Publisher, Inc. All rights reserved.

1. Introduction

Osteoporosis (OP) is a prevalent metabolic structural chronic condition characterized by reduced bone mineral density (BMD), greater bone frailty, diminished bone mass, and a significant vulnerability to fractures resulting from accidents [1]. With one fracture occurring every three seconds and over 1.2 billion individuals affected globally, OP is regarded as a serious global health problem and the most prevalent metabolic bone disorder [2]. It induces over 8.9 million fractures annually. It is essential to comprehend the potential risks and correctly diagnose the condition to raise doctors' knowledge of asymptomatic osteoporosis and to recognize at-risk individuals [3]. Many variables, including sexual identity, aging, body mass index (BMI), height, being underweight, not engaging in appropriate physical fitness, poor nutrition, genetic predisposition, vitamin D and calcium consumption, backache, and other hormonal variables are linked to osteoporosis and are crucial in determining its lifelong diagnosis [4]. Dual-energy X-ray absorption (DXA) is significant in predicting BMD and evaluating bone strength. However, DXA is not always available and fails to depict the state of the bone accurately [5]. Thus, suitable techniques are required for these individuals' surveillance, assessment, and testing [6]. For testing for osteoporosis, several investigators have indeed attempted to create prediction models [7].

Making accurate and conclusive diagnoses and prognoses remain difficult in the healthcare domain. Diagnostic issues are distinctive in that usually call for really precise outcomes. Healthcare professionals analyze patient records the majority of the time. The human diagnosis makes too many mistakes and falls short of social standards. With the development of computer vision technology, healthcare information comprehension has increased, enabling more accurate illness detection. As photos are now potentially saved and distributed, patient records have evolved from being limited to simple assessments [8]. Computer-assisted medical image processing is employed in a variety of clinical uses, including the identification of Alzheimer's illness [9], the identification of small lung nodules [10, 11], and the identification of melanoma using radiography [12]. Radiologists view the results of these technologies as their recommendation [13, 14]. The notion of self-learning, often known as deep learning, has been inspired by the necessity of autonomous systems that possess their intellect and can scoop up characteristics independently.

* Corresponding author.

E-mail address: ms.shivani.batra@gmail.com

The principle of organic training in the central nervous system serves as the foundation for machine learning. Like the brain, many neurons independently pick up information from various sorts of senses and adjust their behaviour to the circumstances. By constructing neural networks that receive certain types of input at the input nodes, the cells in the various levels of the neural network acquire the characteristics on their own and then provide us with the necessary result at the output nodes, and computers imitate the same concept. These networks have accomplished achievements in a variety of sectors, including voice recognition [15], text categorization [16], self-driving technologies [17], and the healthcare industry [18-20]. Such systems incorporate both numerical and visual data. Deep learning refers to using clinical pictures to build more complicated neural networks with several additional intermediary layers to extract the essential data from the pictures. Deep learning has made it possible for systems to carry out their functions without extensive human programming, and they can now make judgments or predictions using information by creating self-learning techniques [21]. In several clinical uses, such as identifying molecular and morphological features [18] and organ segmentation [22], it has produced state-of-the-art findings.

According to previous research, deep learning is thought to be good at classifying features from clinical pictures [8]. Deep Learning (DL) algorithms use high-dimensional parameters to enhance DL systems' efficiency in machine vision and picture categorization. Contrary to deep learning (DL) methods, the machine learning (ML) process relies on explicitly classified characteristics [23, 24]. Deep CNNs have been demonstrated as effective tools for classifying pictures, but because they demand a considerable amount of training datasets, they are challenging to use with clinical radiography datasets. Transfer learning is regarded as an effective technique for deep CNN training whenever the dataset is minimal to avoid overfitting [25].

Several CAD methods involving deep learning at diverse bone locations such as the femur, vertebrae, palm, and teeth are suggested for osteoporosis detection [26]. Nevertheless, little research has been conducted to identify knee osteoporosis. Being the joint that supports posture and balance and facilitates motion, the knee experiences the most strain. Women are more susceptible to tibial and fibular injuries, which raise the prevalence of bone fractures around the knee in an elderly society [27]. A significant 1-year fatality rate of 22% is recorded in senior individuals who suffer femoral injuries, with poorer functioning and bad living conditions [28]. It is anticipated that around 50% of all knee injuries happen in individuals who are over fifty years old. To avoid fractures and save healthcare expenditures, an early diagnosis method is required to determine the incidence of osteoporosis within the knee bone [29].

To identify an early detection method for knee osteoporosis, authors have leveraged the strength of Convolutional networks and the affordability of X-ray scanning in this research. The popular CNNs including, i.e. VGG16 [30], VGG19 [31], Inception V3 [32], Xception [33], DenseNet169 [34], DenseNet201 [34], ResNet101 [35] and ResNet152, [35] are examined in this work to categorize knee X-ray pictures. Following is a summary of our research's substantial achievements:

- Experiments are being investigated for eight well-known CNN networks, i.e., VGG16, VGG19, Inception V3, Xception, DenseNet169, DenseNet201, ResNet101 and ResNet152.
- To investigate the best suitable network for osteoporosis diagnosis in medical settings, transfer learning is performed on all CNN models, and the outcomes are contrasted.
- All CNN networks have transfer learning implemented, and the outcomes are assessed to determine which model is the most effective in detecting osteoporosis in healthcare situations.

The paper is hereafter divided into sections. Section 2 investigates the literature survey. Section 3 discusses various deep learning algorithms explored in current research. Section 4 explains the experiments performed and the results achieved. Section 5 concludes this research.

2. Literature Survey

For osteoporosis diagnosis, the previous investigators employed various imaging techniques, including X-ray absorptiometry, which needed a trajectory for post-processing to calculate the bone mass per unit region. Interpreting the values obtained in the condition of osteoporosis has been made easier by the BMD. The benefits of the simulations are explored and used as the currently available approaches for diagnosing osteoporosis conditions.

A predictive model with two modules has been created by Tang et al. [36] to identify of BMD for osteoporosis diagnosis. The first module locates and separates the area of concern diagnosis, and the second module uses a region of focus characteristics to determine the kind of BMD. Using different lumbar vertebrae, the suggested approach proved effective for segmentation on form retention. The newly created CNN detected the BMD with more precision. The developed model has been able to simulate actual connections with varying effects and has been able to optimize accuracy for complicated data as well.

Nevertheless, the newly created CNN approach used fewer data and took longer to learn the dataset one at the moment.

Liu et al. [37] created a deep U-Net approach for diagnosing and grading osteoporosis. The unedited version has been cataloged and used to create the dataset. The normalized data has been fed to each layer as input to guarantee that the data distribution within every layer is consistent and to speed up learning. Lastly, the data for the forecast have been combined to compute the energy curves. For feature mapping, the forecasting is calculated about the softmax classification created for every pixel. The created U-Net model solved the picture interference issue for the BMD measuring method. The u-Net approach revealed difficulties in localizing and fragmenting the X-ray images since additional training data cycles have been required.

Fang et al. [38] created a deep CNN-based method for measuring BMD and segmenting the bones. The spinal canal segmentation has been done using CNN's U-Net layer, which is a fully linked layer. The vertical bone areas are explicitly indicated as the ground truthfulness to do the analysis. DenseNet 121 has been utilized by the Classifier to calculate BMD. The created approach demonstrated automated detection of osteoporosis, osteopenia, and normal BMD in CT scans. The spinal bones have not been classified using the proposed deep CNN approach. Conventional methodologies could not, however, handle the capability for harmonizing the high-dimensional data and integrating it for non-linear relationships for distinct genetic mutations or classifiers.

Su et al. [39] created a hybrid CNN technique for osteoporosis disease diagnosis using textural characteristics such as the grey-level co-occurrence matrix, local binary pattern, and encoded features. The two types of characteristics were used in X-ray pictures to distinguish between healthy and unwell people. Deep CNN was used to retrieve the CNN features, and handmade features that included a collection of common textural elements were extracted. The created fusion approach performed better at choosing the characteristics to ensure that the data distribution could not skew the outcomes of the analytical techniques. By employing X-ray pictures, the established approach failed to diagnose osteoporosis effectively.

Nazia Fathima et al. [40] created a modified U-Net approach integrating the attention component to monitor osteoporosis. Artificial Neural Networks (ANN) have been utilized in the creation of multiple features-based techniques to create an approach for illness identification. The Dice value across all previous models corroborated the findings for the related datasets, and the built U-Net with attention unit demonstrated noticeably excellent outcomes in terms of precision in classification. The localizing and segmenting the X-ray images using the established U-Net approach revealed constraints.

Computed tomography images were used by Wang et al. [41] to identify osteoporosis in the thoracolumbar spinal column. The correlation between the two observed data is measured using the CT absorbance and fractional bone mass data. The clinical ideal limits have been calculated using the Receiver operator characteristic (ROC) graphs. The elderly and middle-aged individuals were part of the study's demographic. As the model's potential features have been explored, a more considerable computational overhead has been averted by the produced model and cross-validating, the input variables, which selected several parameter combinations for the provided population, used a randomized technique. Unfortunately, the results' capacity to scale across multiple samples has been impacted.

Fang et al. [38] used multi-detector CT scans using CNN information to conduct an early osteoporosis diagnosis. The spinal bone has been segmented using the densely integrated neural network. The post-processed measurements depend on a Quantitative Computed Tomography (QCT) analysis of the benchmarks. The spinal bodies might be automatically excluded from calcification by the model. The spinal structures appeared diverse from the scenario detected, which had a big impact on the diagnosis. The constructed model, however, displayed overfitting due to external validations to the requisite sample.

3. Methodology

The concept driving transfer learning is to apply a framework that has been previously built on a sizable and diverse dataset to employ its generalized domain depiction on an entirely novel issue [42]. This method of learning specifically uses feature maps learned by an algorithm while analyzing pictures, saving both energy and time by not needing to develop the system from the beginning. There are two ways to apply prior expertise to the current work. The primary one treats a pre-trained model as a characteristic harvester by preserving its internal components. A classifier is subsequently taught on top of this preserved framework to ensure knowledge transfer and keep as much data from the prior area as feasible. Typically, the classification model is built employing several dense layers, the final one uses the softmax function to determine the probability distribution over the categories offered, an entirely separate deep learning design, or machine learning techniques like the support vector machine or random forest. Rather, in the subsequent method, the entire design (or a portion) is tailored to the specific job. Essentially, beginning with a random setup, the pre-trained model parameters are employed as a foundation. In most cases, this enables a system to specialize its whole architecture to the new area and obtain training agreements more quickly.

Both approaches can be successful, but in the present study, the authors focus on the first one and evaluate the performance of different systems used as feature extractors. Authors further train the primary classifier element for every framework on the gathered dataset, which operates as a combination of fully connected layers. This training method permits for the emulation of data availability, which is usual whenever novel diseases are first found, while yet allowing for appropriate training of typically data-hungry systems [43]. Authors conducted tests to assess eight renowned ImageNet pre-trained frameworks, i.e., VGG16 [30], VGG19 [31], Inception V3 [32], Xception [33], DenseNet169 [34], DenseNet201 [34], ResNet101 [35] and ResNet152 [35] (as presented in Figure 1) on a combined set obtained from dataset given in [44], which is briefly mentioned later in next section.

- VGG16 and VGG19

Having up to 16 or 19 weight layers, VGGNet was the earliest system to have a deeper layer structure [30, 31]. The investigators could include additional weight layers because of the convolution filters' smaller size. The quantity of weight layers varies according to the design; for example, VGG-16 has thirteen convolution layers and three fully connected levels. Similarly, VGG-19 contains three completely linked layers and sixteen convolution layers. The activation mechanism in the application is ReLU. The VGGNet contains many weight layers, making it hard to learn and bulky (about 550 MB), leading to a long reasoning period.

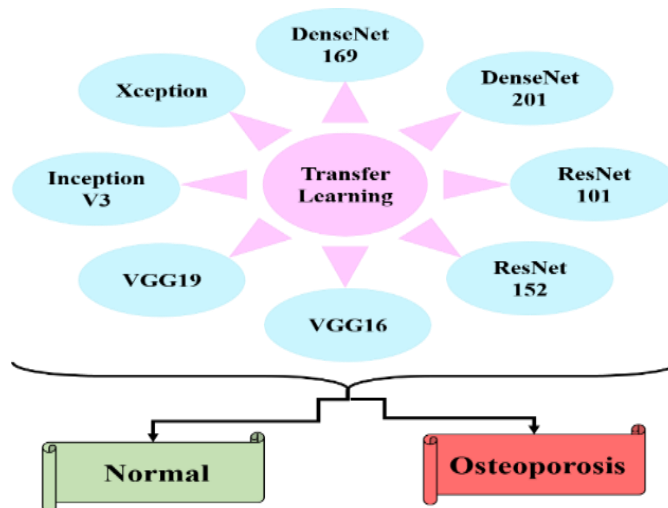


Figure 1. The framework of current research

- Inception V3

One of the fastest-growing deep learning frameworks is Inception v3 [32], which utilizes several enhancements to address issues with earlier Inception algorithms. These enhancements include the incorporation of an additional classifier, factorized convolution procedures, batch normalization, the RMSProp optimizer, and label smoothing. It creates feature maps in various dimensions and layers from an input picture with 299 x 299 x 3 proportions. The Inception v3 inception component allows us to use several feature extraction processes from one particular feature map. These characteristics with different filtering are combined and forwarded to the subsequent layer for more thorough feature extraction.

- Xception

The renowned Inception design [33] served as the model for the Xception framework. On the contrary, Xception uses depth-wise segregated convolution layers to simplify the calculation. A point-wise convolution is used after a depth-wise convolution has been completed to get an outcome with the desired depth. The Xception is made to do these procedures in reverse. Chollet [33] noted that using the ImageNet data set, Xception achieved output efficiency that is identical to Inception-v3. The outcome, nevertheless, shows that the earlier group can do better in different data sets than the latter.

- DenseNet169 and DenseNet201

Huang, Liu, and van der Maaten created the highly interconnected convolutional network, i.e., DenseNet, one of the most profound CNNs [34]. In contrast to a conventional CNN, DenseNet transmits the input picture through many convolutional layers, with every layer and sharing its feature maps to all succeeding layers across channel-wise conjunction. The theory is that each layer acquires "collective learning" from all levels that came before it. As a result, the planned network structure

may be less complicated and more tightly packed, resulting in improved processing and storage performance. Each layer acquires characteristics from all previous levels. The DenseNet169 and DenseNet201 versions were used in this investigation, wherein the depth of the ImageNet models is indicated by an integer associated with every version. Every DenseNet version requires an input picture of $224 * 224 * 3$ color lines.

- ResNet101 and ResNet152

The Microsoft research group created ResNet to make learning deeper neural systems easier. ResNets' basic principle is to use short links to acquire the cumulative residual value via identity mapping [35]. Variations with 18, 34, 50, 101, and 152 weight layers are available. The ResNet101 and ResNet152 variants have been utilized in this investigation. ResNet designs use input layers to implement residual procedures rather than non-discriminatory procedures. ResNet designs, in contrast to VGG, have quick connections applied in feed-forward neural networks. Quick links do not add additional settings or increase computing overhead. This allows for transmitting pertinent data from the preceding layer to the subsequent layers [35]. In opposition to VGG designs, ResNet topologies have a fully connected layer at the network's conclusion and a global average pooling layer. In the global average pooling procedure, the mean result in every attribute map is moved to the following layer without a dropout procedure.

4. Experiment and Results

For testing purposes, authors examined the effectiveness of eight CNN designs for identifying osteoporosis in knee x-rays: VGG16 [30], VGG19 [31], Inception V3 [32], Xception [33], DenseNet169 [34], DenseNet201 [34], ResNet101 [35] and ResNet152 [35]. To determine if transfer learning could boost classification effectiveness, the CNN models had been initially trained on the provided osteoporosis dataset, after which transfer learning was used leveraging the pre-trained networks developed on the ImageNet dataset, which contains millions of pictures. The dataset is publicly available on Kaggle [44]. The dataset constituted a total of 372 images, of which 186 images belong to the regular class and the rest belong to osteoporosis.

4.1. Performance Evaluation Metrics

To assess the performance of various models, various evaluation parameters are considered i.e., accuracy curve, loss curve, confusion matrix and comparative analysis of average accuracy, precision, recall, and f1-score.

- Accuracy Curve

The model's accuracy curves demonstrate how effectively it collects and comprehends information. Overfitting is present when there is a discrepancy in accuracy across training and testing. The overfitting increases as the gap widens. Figure 2 reflects various accuracy graphs achieved by underlying models.

- Loss Curve

The loss graphs display the training duration and model inclination. A sizable gap between the train and test lines demonstrates the growth spectrum with training. Figure 3 presents various loss graphs achieved by underlying models.

- Confusion Matrix

The confusion matrix (CM) is a technique for summarizing the efficacy of a system for classification. It identifies the general errors the classifier is committing and details the individual errors. The confusion matrix helps the restriction of relying solely on classification accuracy. Figure 4 depicts the confusion matrix of various underlying models.

- Precision, Recall and F1-Score

Precision refers to how accurate/precise a model is regarding the number of desirable results it correctly predicted. If the expenses of False Positive are huge, precision is a suitable metric to assess. The recall is the proportion of "genuine positives" that our system can identify by classifying them as "positive." When attempting to strike an equilibrium between accuracy and recall, the F1-score, which is an expression of both, is required. Figure 5 presents a comparative analysis of average accuracy, precision, recall, and f1-score achieved by various underlying models.

4.2. Discussion

The eight CNN models explored in this research are VGG16 [30], VGG19 [31], Inception V3 [32], Xception [33], DenseNet169 [34], DenseNet201 [34], ResNet101 [35] and ResNet152 [35] has performed exceptionally well in classifying osteoporosis. However, the lowest accuracy is recorded by ResNet101, i.e., 81.82%. Further, it has been observed that VGG16 has outperformed other models in all parameters (accuracy, precision, recall and f1-score).

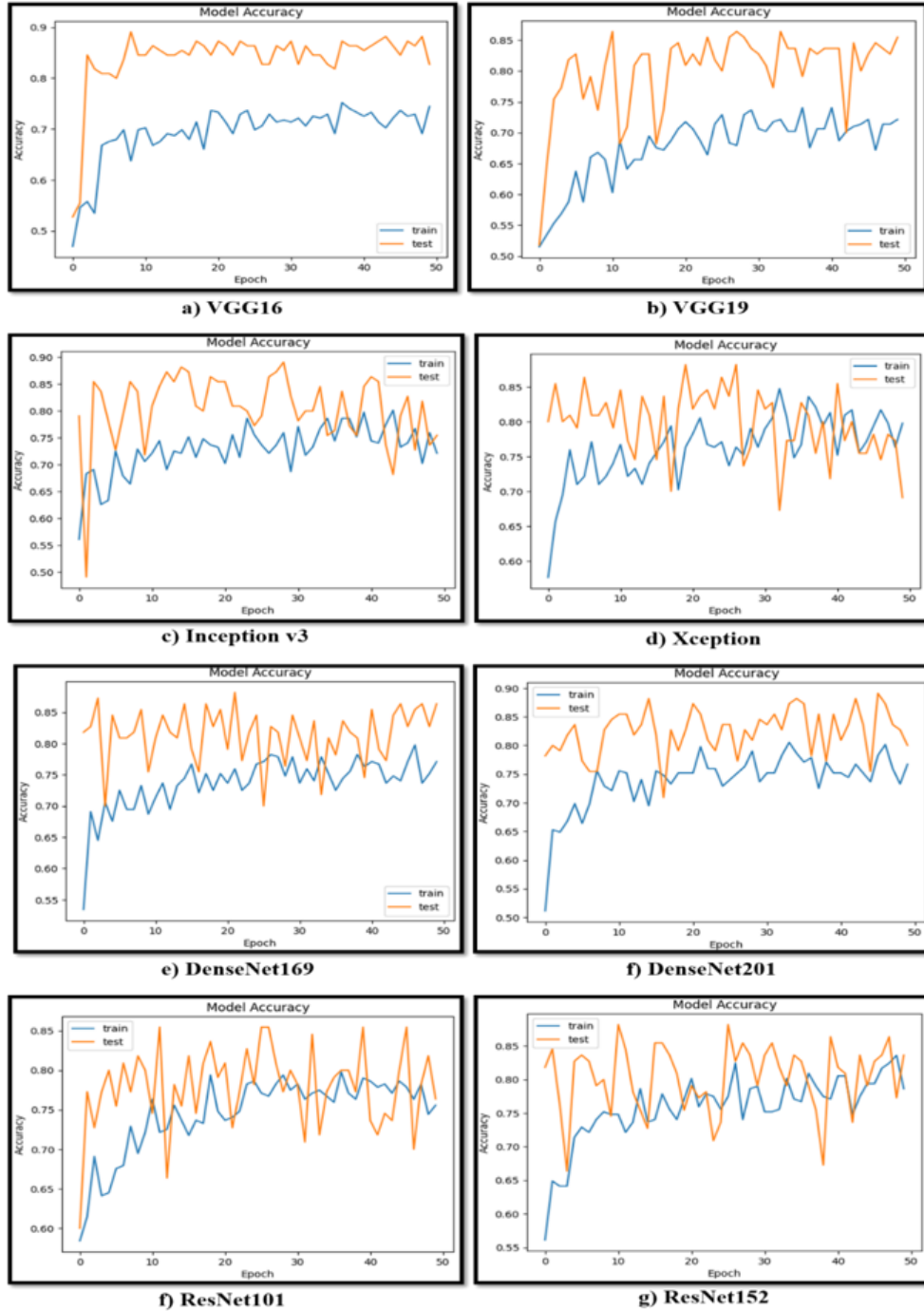


Figure 2. Accuracy achieved by various underlying deep learning models

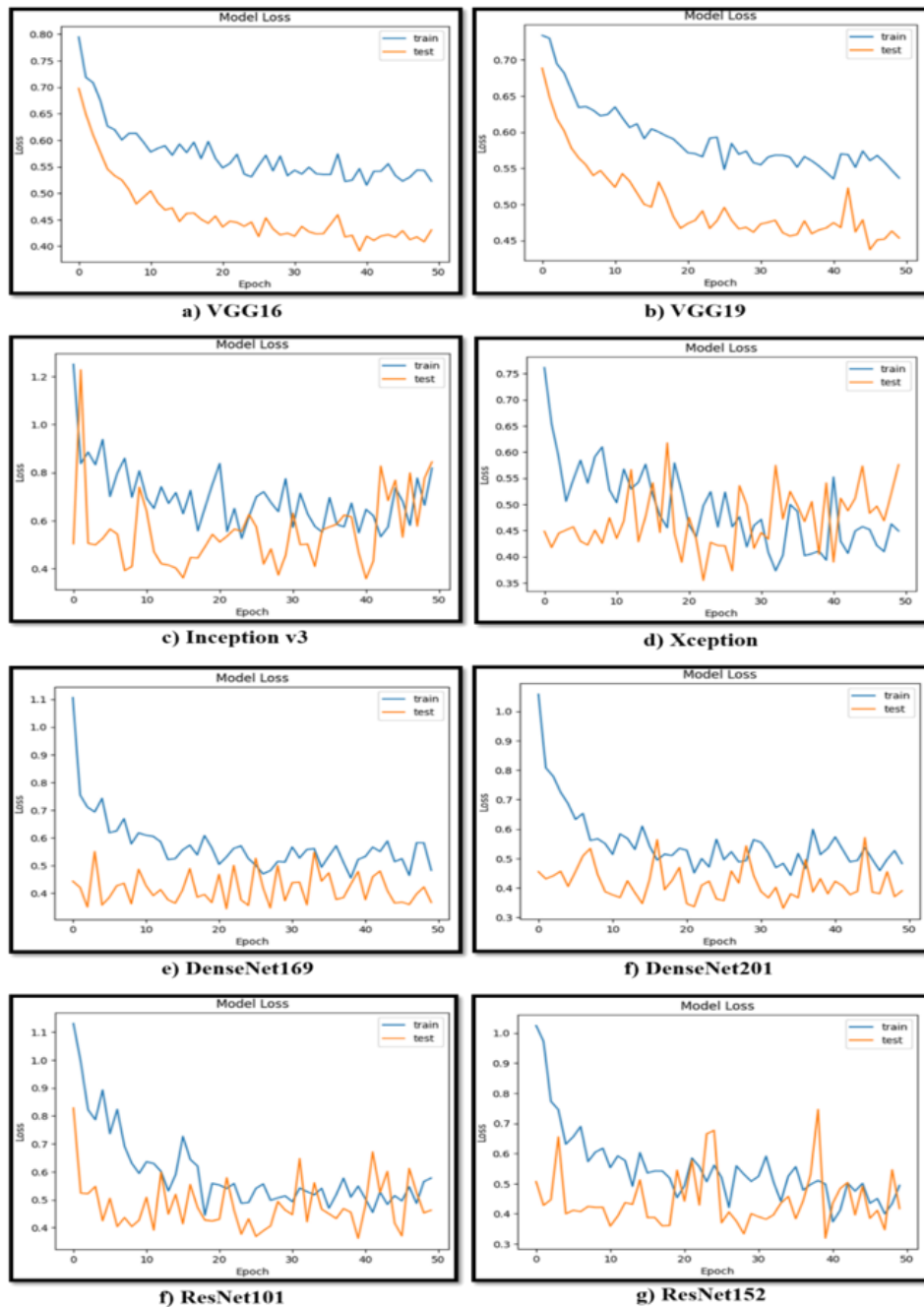


Figure 3. Loss incurred by various underlying deep learning models

After VGG16, the DenseNet169 model has shown the highest performance. Further, the performance of VGG19 and Inception V3 has been comparable. For a deep learning model to be effective, enormous volumes of data are needed. A limitation of the investigation is the insufficiently high number of training images in the dataset. These restrictions can be reduced, though, by using data augmentation. Osteoporosis is brought on by several variables, including age, gender, height, body mass index, and others, in addition to poor bone mineral density. These osteoporosis indicators are crucial from a clinical standpoint. In future research, authors aim to improve the techniques by using patient characteristics as clinical covariates, such as age and gender, to build an ensemble model incorporating the transfer learning models.

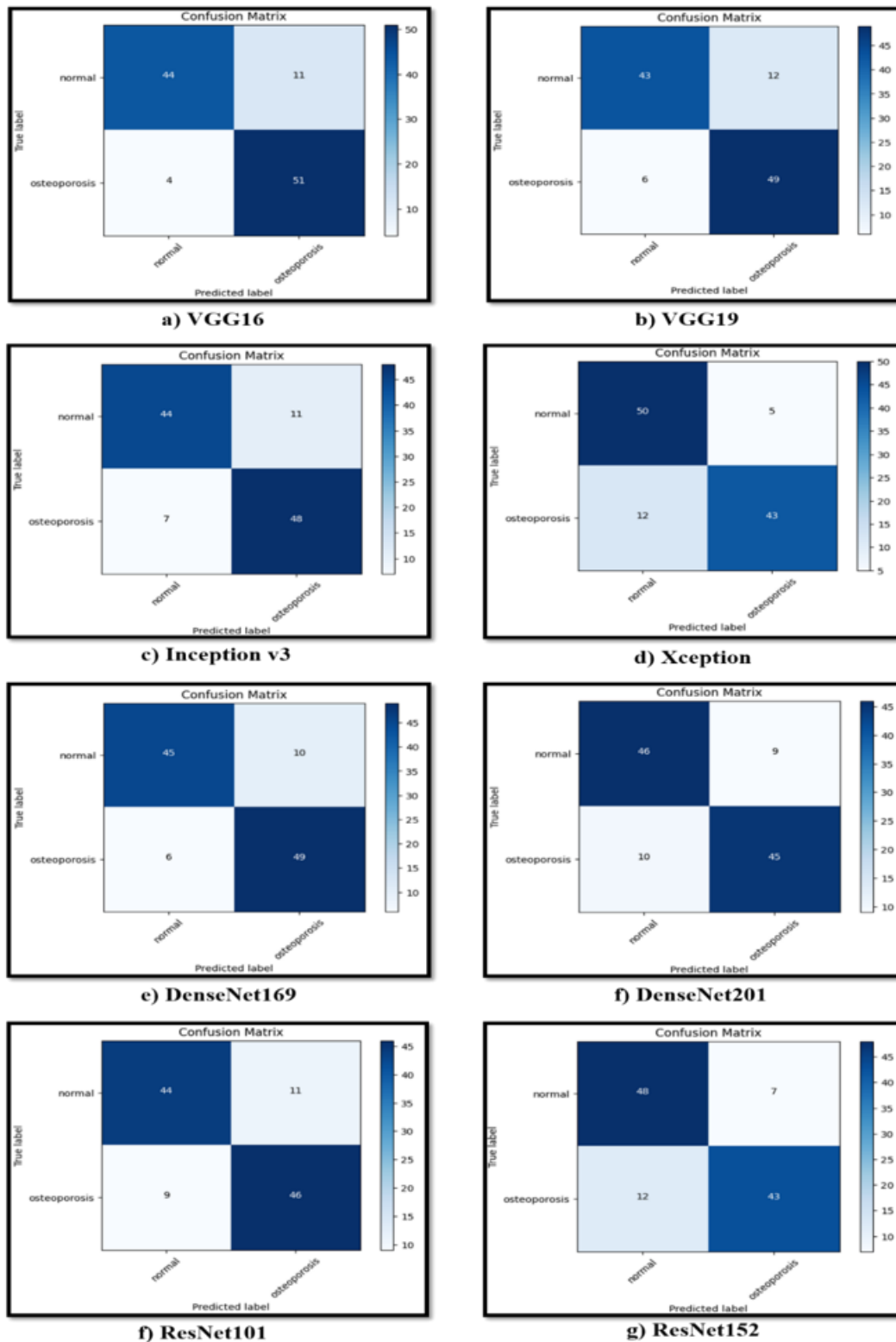


Figure 4. Confusion matrix achieved by various underlying deep learning models

5. Conclusion

Osteoporosis is a chronic illness affecting people all over the globe and can result in permanent impairment, catastrophic injuries, excruciating pain, and even early death. Deep learning techniques for risk group prediction can benefit the economy and ease the strain on healthcare services.

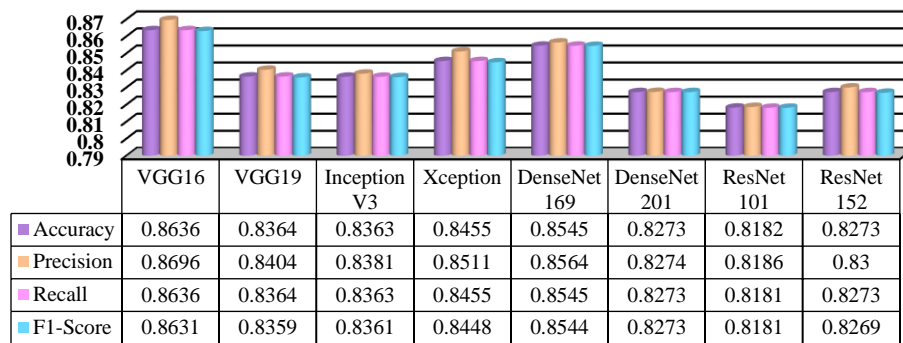


Figure 5. Performance evaluation of various underlying deep learning models

In the current research, authors analyzed and contrasted the efficiency of well-known CNN architectures for osteoporosis diagnosis from knee X-ray pictures, including VGG16, VGG19, Inception V3, Xception, DenseNet169, DenseNet201, ResNet101, and ResNet152. The X-ray pictures utilized have been retrieved from a publicly accessible dataset split into groups for people with osteoporosis and those without. There were 372 overall knee x-ray images in the dataset. The findings demonstrate that ResNet101 had the lowest efficiency (81.82% accuracy), while VGG16 had the highest score (86.36% accuracy). The conclusions of all CNNs demonstrated good diagnostic accuracy and indicated that osteoporosis may be accurately diagnosed through a knee X-ray employing transfer learning and CNN. The current study's findings showed that deep learning techniques can locate relevant sports procedures with satisfactory results, and by implementing these techniques in medical practice, both doctors and patients may readily profit.

References

- [1] Sirufo, M.M., De Pietro, F., Bassino, E.M., Ginaldi, L., and De Martinis, M. Osteoporosis in Skin Diseases. *International Journal of Molecular Sciences*, vol. 21, no. 13, pp. 4749, 2020.
- [2] Hussein, R.S. and Wahdan, M.M. Knowledge About Symptoms and Risk Factors of Osteoporosis Among Adult Women in Cairo, *The Egyptian Journal of Community Medicine*, vol. 39, no. 2, 2021.
- [3] Ou Yang, W.Y., Lai, C.C., Tsou, M.T., and Hwang, L.C. Development of Machine Learning Models for Prediction of Osteoporosis from Clinical Health Examination Data. *International journal of environmental research and public health*, vol. 18, no. 14, pp. 7635, 2021.
- [4] Aspray, T.J. and Hill, T.R. Osteoporosis and the Ageing Skeleton. *Biochemistry and cell biology of ageing: Part II clinical science*, pp. 453-476, 2019.
- [5] Ross, R., Chaput, J.P., Giangregorio, L.M., Janssen, I., Saunders, T.J., Kho, M.E., Poitras, V.J., Tomasone, J.R., El-Kotob, R., McLaughlin, E.C., and Duggan, M. Canadian 24-Hour Movement Guidelines for Adults Aged 18–64 Years and Adults Aged 65 Years or Older: An Integration of Physical Activity, Sedentary Behaviour, and Sleep. *Applied Physiology, Nutrition, and Metabolism*, vol. 45, no. 10, pp. S57-S102, 2020.
- [6] Asadipooya, K., Abdalbary, M., Ahmad, Y., Kakani, E., Monier-Faugere, M.C. and El-Husseini, A. Bone Quality in CKD Patients: Current Concepts and Future Directions–Part I. *Kidney Diseases*, vol. 7, no. 4, pp. 268-277, 2021.
- [7] Forgetta, V., Keller-Baruch, J., Forest, M., Durand, A., Bhatnagar, S., Kemp, J.P., Nethander, M., Evans, D., Morris, J.A., Kiel, D.P. and Rivadeneira, F. Development of a Polygenic Risk Score to Improve Screening for Fracture Risk: A Genetic Risk Prediction Study. *PLoS medicine*, vol. 17, no. 7, pp. e1003152, 2020.
- [8] Litjens, G., Kooi, T., Bejnordi, B.E., Setio, A.A.A., Ciompi, F., Ghafoorian, M., Van Der Laak, J.A., Van Ginneken, B., and Sánchez, C.I. A Survey on Deep Learning in Medical Image Analysis. *Medical image analysis*, vol. 42, pp. 60-88, 2017.
- [9] Padilla, P., López, M., Górriz, J.M., Ramirez, J., Salas-Gonzalez, D., and Alvarez, I. NMF-SVM Based CAD Tool Applied to Functional Brain Images for the Diagnosis of Alzheimer's Disease. *IEEE Transactions on medical imaging*, vol. 31, no. 2, pp. 207-216, 2011.
- [10] Li, Q. Recent Progress in Computer-Aided Diagnosis of Lung Nodules on Thin-Section CT. *Computerized Medical Imaging and Graphics*, vol. 31, no. 4-5, pp. 248-257, 2007.
- [11] Batra, S., Sharma, H., Boulila, W., Arya, V., Srivastava, P., Khan, M.Z., and Krichen, M. An Intelligent Sensor Based Decision Support System for Diagnosing Pulmonary Ailment through Standardized Chest X-Ray Scans. *Sensors*, vol. 22, no. 19, pp. 7474, 2022.
- [12] Birdwell, R.L., Bandothkar, P., and Ikeda, D.M. Computer-Aided Detection with Screening Mammography in a University Hospital Setting. *Radiology*, vol. 236, no. 2, pp. 451-457, 2005.
- [13] Doi, K. Computer-Aided Diagnosis in Medical Imaging: Historical Review, Current Status and Future Potential. *Computerized medical imaging and graphics*, vol. 31, no. 4-5, pp. 198-211, 2007.
- [14] Sachdeva, S., Batra, D., and Batra, S. Storage Efficient Implementation of Standardized Electronic Health Records Data. In *2020 IEEE International Conference on Bioinformatics and Biomedicine (BIBM)*, IEEE, pp. 2062-2065, 2020.
- [15] Hinton, G., Deng, L., Yu, D., Dahl, G.E., Mohamed, A.R., Jaitly, N., Senior, A., Vanhoucke, V., Nguyen, P., Sainath, T.N., and Kingsbury, B. Deep Neural Networks for Acoustic Modeling in Speech Recognition: The Shared Views of Four Research Groups. *IEEE Signal processing magazine*, vol. 29, no. 6, pp. 82-97, 2012.

- [16] Chen, L., Wang, S., Fan, W., Sun, J., and Naoi, S. Beyond Human Recognition: A CNN-Based Framework for Handwritten Character Recognition. In *2015 3rd IAPR Asian Conference on Pattern Recognition (ACPR)*, IEEE, pp. 695-699, 2015.
- [17] Teichmann, M., Weber, M., Zoellner, M., Cipolla, R., and Urtasun, R. Multinet: Real-Time Joint Semantic Reasoning for Autonomous Driving. In *2018 IEEE intelligent vehicles symposium (IV)*, IEEE, pp. 1013-1020, 2018.
- [18] Pereira, S., Pinto, A., Alves, V., and Silva, C.A. Brain Tumor Segmentation using Convolutional Neural Networks in MRI Images. *IEEE transactions on medical imaging*, vol. 35, no. 5, pp. 1240-1251, 2016.
- [19] Batra, S. and Sachdeva, S. Organizing Standardized Electronic Healthcare Records Data for Mining. *Health Policy and Technology*, vol. 5, no. 3, pp. 226-242, 2016.
- [20] Batra, S., Khurana, R., Khan, M.Z., Boulila, W., Koubaa, A., and Srivastava, P. A Pragmatic Ensemble Strategy for Missing Values Imputation in Health Records. *Entropy*, vol. 24, no. 4, pp. 533, 2022.
- [21] Liu, W., Wang, Z., Liu, X., Zeng, N., Liu, Y., and Alsaadi, F.E. A Survey of Deep Neural Network Architectures and Their Applications. *Neurocomputing*, vol. 234, pp. 11-26, 2017.
- [22] Esteva, A., Kuprel, B., Novoa, R.A., Ko, J., Swetter, S.M., Blau, H.M., and Thrun, S. Dermatologist-Level Classification of Skin Cancer with Deep Neural Networks. *nature*, vol. 542, no. 7639, pp. 115-118, 2017.
- [23] Abubakar, U.B., Boukar, M.M., and Adeshina, S. Evaluation of Parameter Fine-Tuning with Transfer Learning for Osteoporosis Classification in Knee Radiograph. *International Journal of Advanced Computer Science and Applications*, vol. 13, no. 8, 2022.
- [24] Pathak, A., Batra, S., and Sharma, V. An Assessment of the Missing Data Imputation Techniques for Covid-19 Data. In *Proceedings of 3rd International Conference on Machine Learning, Advances in Computing, Renewable Energy and Communication: MARC 2021*, Singapore: Springer Nature Singapore, pp. 701-706, 2022.
- [25] Lee, K.S., Jung, S.K., Ryu, J.J., Shin, S.W., and Choi, J. Evaluation of Transfer Learning with Deep Convolutional Neural Networks for Screening Osteoporosis in Dental Panoramic Radiographs. *Journal of clinical medicine*, vol. 9, no. 2, pp. 392, 2020.
- [26] Wani, I.M. and Arora, S. Computer-Aided Diagnosis Systems for Osteoporosis Detection: A Comprehensive Survey. *Medical & biological engineering & computing*, vol. 58, pp. 1873-1917, 2020.
- [27] Court-Brown, C.M. and Caesar, B. Epidemiology of Adult Fractures: A Review. *Injury*, vol. 37, no. 8, pp. 691-697, 2006.
- [28] Stange, R. and Raschke, M.J. Osteoporotic Distal Femoral Fractures: When to Replace and How. *Surgical and Medical Treatment of Osteoporosis: Principles and Practice*, pp. 235-244, 2020.
- [29] Wang, S.P., Wu, P.K., Lee, C.H., Shih, C.M., Chiu, Y.C., and Hsu, C.E. Association of Osteoporosis and Varus Inclination of the Tibial Plateau in Postmenopausal Women with Advanced Osteoarthritis of the Knee. *BMC Musculoskeletal Disorders*, vol. 22, pp. 1-8, 2021.
- [30] Nijaguna, G.S., Babu, J.A., Parameshachari, B.D., de Prado, R.P., and Frnda, J. Quantum Fruit Fly Algorithm and ResNet50-VGG16 for Medical Diagnosis. *Applied Soft Computing*, vol. 136, pp. 110055, 2023.
- [31] Bansal, M., Kumar, M., Sachdeva, M., and Mittal, A. Transfer Learning for Image Classification using VGG19: Caltech-101 Image Data Set. *Journal of ambient intelligence and humanized computing*, pp. 1-12, 2021.
- [32] Kumar, S., Gupta, S.K., Kaur, M., and Gupta, U. VI-NET: A Hybrid Deep Convolutional Neural Network using VGG and Inception V3 Model for Copy-Move Forgery Classification. *Journal of Visual Communication and Image Representation*, vol. 89, pp. 103644, 2022.
- [33] Chollet, F. Xception: Deep Learning with Depthwise Separable Convolutions. In *Proceedings of the IEEE conference on computer vision and pattern recognition*, pp. 1251-1258, 2017.
- [34] Huang, G., Liu, Z., Van Der Maaten, L., and Weinberger, K.Q. Densely Connected Convolutional Networks. In *Proceedings of the IEEE conference on computer vision and pattern recognition*, pp. 4700-4708, 2017.
- [35] He, K., Zhang, X., Ren, S., and Sun, J. Deep Residual Learning for Image Recognition. In *Proceedings of the IEEE conference on computer vision and pattern recognition*, pp. 770-778, 2016.
- [36] Tang, C., Zhang, W., Li, H., Li, L., Li, Z., Cai, A., Wang, L., Shi, D., and Yan, B. CNN-Based Qualitative Detection of Bone Mineral Density via Diagnostic CT Slices for Osteoporosis Screening. *Osteoporosis International*, vol. 32, pp. 971-979, 2021.
- [37] Liu, J., Wang, J., Ruan, W., Lin, C., and Chen, D. Diagnostic and Gradation Model of Osteoporosis Based on Improved Deep U-Net Network. *Journal of medical systems*, vol. 44, pp. 1-7, 2020.
- [38] Fang, Y., Li, W., Chen, X., Chen, K., Kang, H., Yu, P., Zhang, R., Liao, J., Hong, G., and Li, S. Opportunistic Osteoporosis Screening in Multi-Detector CT Images using Deep Convolutional Neural Networks. *European Radiology*, vol. 31, pp. 1831-1842, 2021.
- [39] Su, R., Liu, T., Sun, C., Jin, Q., Jennane, R., and Wei, L. Fusing Convolutional Neural Network Features with Hand-Crafted Features for Osteoporosis Diagnoses. *Neurocomputing*, vol. 385, pp. 300-309, 2020.
- [40] Nazia Fathima, S.M., Tamilselvi, R., Parisa Beham, M., and Sabarinathan, D. Diagnosis of Osteoporosis using Modified U-Net Architecture with Attention Unit in DEXA and X-Ray Images. *Journal of X-Ray Science and Technology*, vol. 28, no. 5, pp. 953-973, 2020.
- [41] Wang, P., She, W., Mao, Z., Zhou, X., Li, Y., Niu, J., Jiang, M., and Huang, G. Use of Routine Computed Tomography Scans for Detecting Osteoporosis in Thoracolumbar Vertebral Bodies. *Skeletal Radiology*, vol. 50, pp. 371-379, 2021.
- [42] Pan, S.J. and Yang, Q. A Survey on Transfer Learning. *IEEE Transactions on knowledge and data engineering*, vol. 22, no. 10, pp. 1345-1359, 2009.
- [43] Cheplygina, V., de Bruijne, M., and Pluim, J.P. Not-So-Supervised: A Survey of Semi-Supervised, Multi-Instance, and Transfer Learning in Medical Image Analysis. *Medical image analysis*, vol. 54, pp. 280-296, 2019.
- [44] Osteoporosis Knee X-ray Dataset, <https://www.kaggle.com/datasets/stevepython/osteoporosis-knee-xray-dataset>, accessed on December 1, 2023.